Ab initio calculation of optical second harmonic generation at the rutile TiO_2(110) surface

H. Sano* and G. Mizutani
School of Materials Science, Japan Advanced Institute of Science and Technology, Tatsunokuchi, Ishikawa 923-1292, Japan

W. Wolf
Materials Design s.a.r.l., 44, av. F. -A. Bartholdi, 72000 Le Mans, France

R. Podloucky
Institute of Physical Chemistry, University of Vienna, Liechtensteinstrasse 22A, A-1090 Vienna, Austria and Center of Computational Materials Science, Gumpendorferstrasse 1a, A-1060 Vienna, Austria

(Received 11 April 2004; published 15 September 2004)

Optical second harmonic (SH) response of rutile TiO_2(110) surface was studied by the self-consistent full potential linearized augmented plane-wave method within the local-density approximation. The calculated SH response of the relaxed surface agrees with the measured SH intensity as a function of the excitation photon energy and the sample rotation angle around its surface normal. In order to clarify the origin of the large surface SH response at the SH photon energy of about $2\hbar\omega = 4$ eV, SH intensities from various Ti-O bonds on the surface were calculated. The result revealed that the zigzag chains consisting of bridging oxygen and neighboring sixfold coordinated titanium atoms on the top surface layer dominantly contribute to the SH response of the TiO_2(110) surface.

DOI: 10.1103/PhysRevB.70.125411 PACS number(s): 78.68.+m, 78.20.Bh, 42.65.Ky

I. INTRODUCTION

Titanium dioxide (TiO_2) has attracted much attention as a material with useful properties, e.g., photocatalysis and its related properties such as photoassisted degradation of organic molecules and photocatalytic super-hydrophilicity. For clarifying the mechanism of catalytic and degradation reactions, it is very important to know basic properties of TiO_2 surfaces such as surface structure and surface electronic states.

There are numerous studies on TiO_2 surfaces reported in the literature.[1] The structure of several TiO_2 surfaces was investigated by x-ray diffraction (XRD),[2] ion scattering,[3,4] scanning tunnel microscopy,[5] and atomic force microscopy.[6] As a result, the structure of the rutile (1×1) TiO_2(110) stoichiometric surface is accurately characterized. The electronic states of the TiO_2 surfaces were measured by photoemission spectroscopy,[7,8] inverse photoemission spectroscopy,[9] and x-ray absorption spectroscopy.[10] In addition to these experimental studies, optical second harmonic generation (SHG) has been used to analyze the electronic states of TiO_2 surfaces.[11–15] SHG is not only sensitive to the surface electronic structure, but also has attractive advantages such as high spectral resolution, nondestructive character, and insensitivity to ambient gas or liquid. Therefore, SHG can be used for *in situ* observation of surface electronic states of a TiO_2 sample showing catalytic activity in air or solution.

The SHG experiments for TiO_2 surfaces[13–15] have shown some outstanding results: the anisotropy of the SH response in the surface plane depends drastically on the incident photon energy, and the surface band gap estimated from a resonant peak in the SH intensity spectra is slightly larger than the bulk band gap. However, the interpretation of the experimental SHG data remained unsufficient, because of lacking knowledge on the underlying electronic transitions. Therefore, reliable *ab initio* calculations of the surface SH response are needed in order to understand the results of SHG experiments.

Ab initio calculations of the surface SH response were so far performed only for a few surface systems of metals and elemental semiconductors such as Si.[16–21] In the case of TiO_2, there have been a lot of theoretical studies on bulk electronic states, bulk linear optical properties,[22,23] surface structure, and surface electronic states.[24–29] However, calcu-

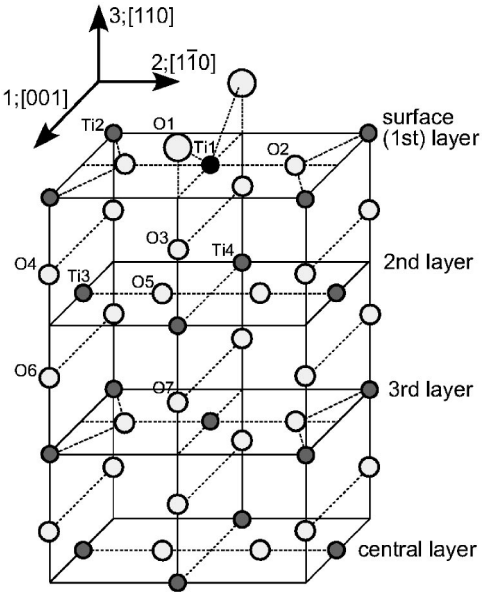

FIG. 1. Upper half of the rutile TiO_2(110) slab for the calculation.

TABLE I. The atomic displacements from bulk terminated positions and bond lengths of rutile (1×1) $TiO_2(110)$ surface. The labels and directions refer to Fig. 1.

Label	PAW-GGA (this work)	PP-LDA[a]	PP-GGA[b]	FLAPW-GGA[c]	Exp-SXRD[d]
Displacement (Å)					
Ti(1) [110]	0.20	0.13	0.23	0.08	0.12±0.05
Ti(2) [110]	−0.17	−0.17	−0.11	−0.23	−0.16±0.05
Ti(3) [110]	−0.077	−0.079	−0.06	−0.13	−0.09±0.04
Ti(4) [110]	0.12	0.063	0.12	0.07	0.07±0.04
O(1) [110]	−0.005	−0.063	−0.02	−0.16	−0.27±0.08
O(2) [110]	0.16	0.13	0.18	0.09	0.05±0.05
$[1\bar{1}0]$	0.053	0.037	0.05	0.06	0.16±0.08
O(3) [110]	−0.012	−0.074	0.03	−0.09	0.05±0.08
O(4) [110]	0.013	0.015	0.03	−0.05	0.00±0.08
O(5) [110]	0.01	−0.026	0	−0.04	0.02±0.06
$[1\bar{1}0]$	−0.033	−0.047	0.02	−0.03	0.07±0.06
O(6) [110]	0.008	−0.01	0.03	−0.04	−0.09±0.08
O(7) [110]	0.004		0	−0.07	−0.12±0.07
Bond length (Å)					
Ti(1)-O(1)	1.82	1.80	1.80	1.80	1.71±0.07
Ti(1)-O(2)	2.03	2.02	2.04	2.00	2.15±0.09
Ti(1)-O(3)	2.09	2.06	2.09	2.06	1.99±0.09
Ti(2)-O(2)	1.94	1.92	1.94	1.94	1.84±0.05
Ti(2)-O(4)	1.80	1.80	1.85	1.86	1.84±0.13

[a]Reference 25.
[b]Reference 27.
[c]Reference 29.
[d]Reference 2.

lations of the SH response of the TiO_2 surface have not yet been reported.

In the present study, we show calculated data of surface SHG of the rutile $TiO_2(110)$ by using the self-consistent full potential linearized augmented plane-wave (FLAPW) method.[30,31] The (110) face was chosen because the basic properties of this most stable rutile surface have been intensively studied[1] and sufficient experimental data[15] are available for comparison with calculated results. Our calculations agree well with the experimental results of the SH intensity as a function of the excitation photon energy and the sample rotation angle around its surface normal.[15] The theoretical analysis indicates that the zigzag chains consisting of bridging oxygen and neighboring sixfold coordinated titanium atoms dominantly contribute to the strong SH response at the SH photon energy of $2\hbar\omega=4$ eV.

II. COMPUTATIONAL ASPECTS

For modeling the rutile (1×1) $TiO_2(110)$ stoichiometric, defect free surface, we applied a repeated slab model. The unit cell contains 7 (Ti_2O_4) layers as shown in Fig. 1, and the thickness of the vacuum layer above the top surface is 8.47 Å. The structure of the relaxed $TiO_2(110)$ surface was calculated by the projector augmented wave (PAW) method within the generalized gradient approximation (GGA) as implemented in the Vienna Ab initio Simulation Package (vasp).[32] Table I compares the atomic displacements and bond lengths of the optimized surface geometry to the data obtained from a surface XRD experiment[2] and other calculations.[25,27,29] Our calculated bond lengths of the relaxed surface are in good agreement with the experimental data and other calculated results, although in particular the displacement of the bridging oxygen shows some consistent discrepancy between the measurements and all calculations. In addition to the relaxed surface, calculations were also performed for the unrelaxed (bulk truncated) surface in order to reveal the effect of the surface structure on the SH response.

The calculation of the electronic states and the optical properties was performed by the FLAPW method within the local-density approximation (LDA) of Hedin and Lundqvist.[33,34] For Ti the semi-core 3*s* and 3*p* states were treated in a second energy window.[35] The number of basis functions was restricted to about 100 per atom by chosing a momentum cutoff of 4.0 a.u.$^{-1}$ Density, potential, and basis functions inside the atomic spheres were expanded into spherical harmonics up to $l_{max}=8$. A regular mesh of 32 special $\boldsymbol{k}$ points in the irreducible part of the two-dimensional surface Brillouin zone was chosen, generated by $15\times7\times1$ Monkhorst-Pack parameters.[36] The radii of the atomic spheres were chosen as $r(O)=1.68$ a.u. for oxygen and $r(Ti)=1.90$ a.u. for titanium for most atomic sites in the slab, and slightly smaller radii of $r(O)=1.60$ a.u. and $r(Ti)$

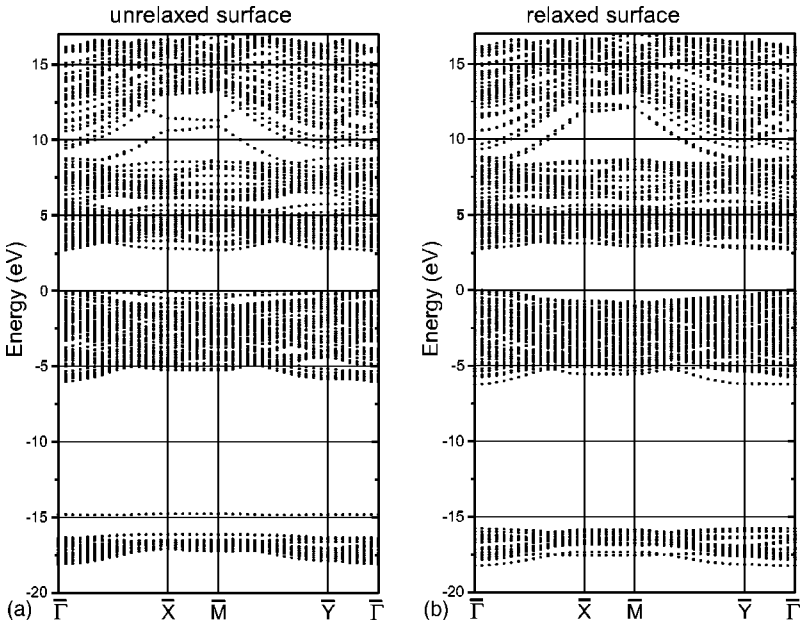

FIG. 2. Surface electronic band structures of (a) unrelaxed and (b) relaxed $TiO_2(110)$ surfaces. The band gap is increased by a scissors operator with $\Delta_{QP}=1.5$ eV.

$=1.79$ a.u. were set for some atomic sites in the relaxed surface region.

Details of the calculation method of the linear and nonlinear optical susceptibilities are described in our previous paper.[20] The optical response was calculated within the electric dipole approximation, and excitonic and local-field effects are not considered in the present calculation. Five nonlinear optical susceptibility components $\chi^{(2)}_{113}$, $\chi^{(2)}_{223}$, $\chi^{(2)}_{311}$, $\chi^{(2)}_{322}$, and $\chi^{(2)}_{333}$ were obtained, where the coordinate axes 1, 2, and 3 represent the [001], $[1\bar{1}0]$, and [110] directions, respectively. The other susceptibility components are zero due to the selection rules for the C_{2v} symmetry of the (1×1) $TiO_2(110)$ surface.

Within standard density-functional theory calculated band gaps are typically smaller than experimental data, leading to red-shifted optical spectra. As an improvement, quasiparticle (QP) corrections have been used, such as Hedin's *GW* approximation,[37] where the self energy operator is expressed as convolution of the single-particle propagator *G* and the dynamically screened Coulomb interaction *W*. However, this is beyond the scope of this study, because of the enormous computational demands required for a large TiO_2 slab system. Instead, a scissors operator scheme was used in the present calculation. The scissors operator shifts all the conduction bands upward rigidly by the constant energy shift Δ_{QP}, leaving the band topology unchanged. When applying the scissors operator in the SHG calculation, we shifted only the energies, and did not renormalize the momentum matrix elements. Without the renormalization, spectral intensities are slightly underestimated.[38] However, this underestimation is insignificant for our discussion because in this study we do not focus on absolute SH intensities but on their dependence on various parameters such as incident photon energy, polarization configuration, and sample rotation angle. The value of $\Delta_{QP}=1.5$ eV was chosen to match the calculated optical absorption edge with the measured one.

In order to enable direct comparison with the measured SHG data, the SH intensity was calculated from the nonlinear optical susceptibility by using the three-layer model[12] for considering the dielectric screening effect on the electric field. In the three-layer model, a vacuum layer, a very thin surface layer with the SHG activity, and a bulk layer are considered. The very thin surface layer is assumed to have the nonlinear susceptibility calculated by the *ab initio*

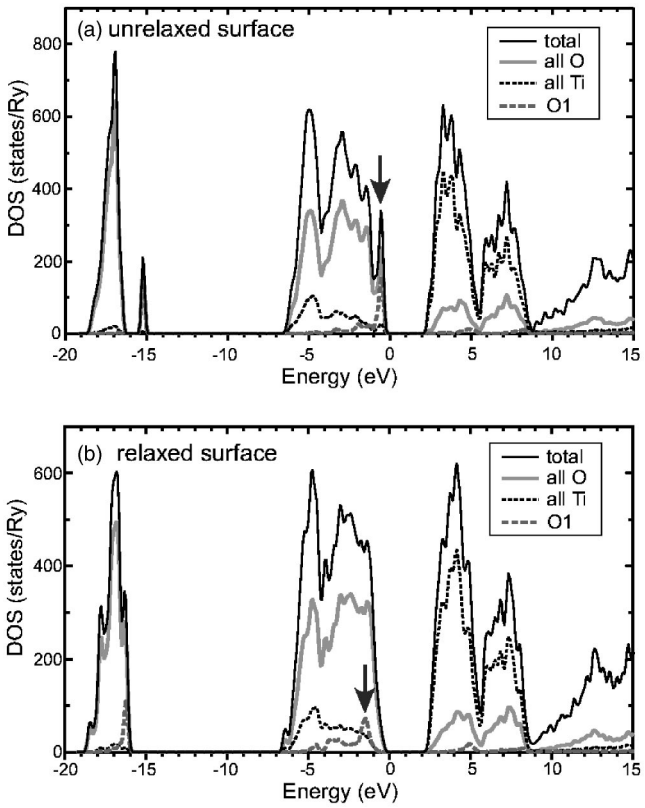

FIG. 3. Density of states of (a) unrelaxed and (b) relaxed $TiO_2(110)$ surfaces. O1 represents the bridging oxygen on the surface. The band gap is increased by a scissors operator with $\Delta_{QP}=1.5$ eV.

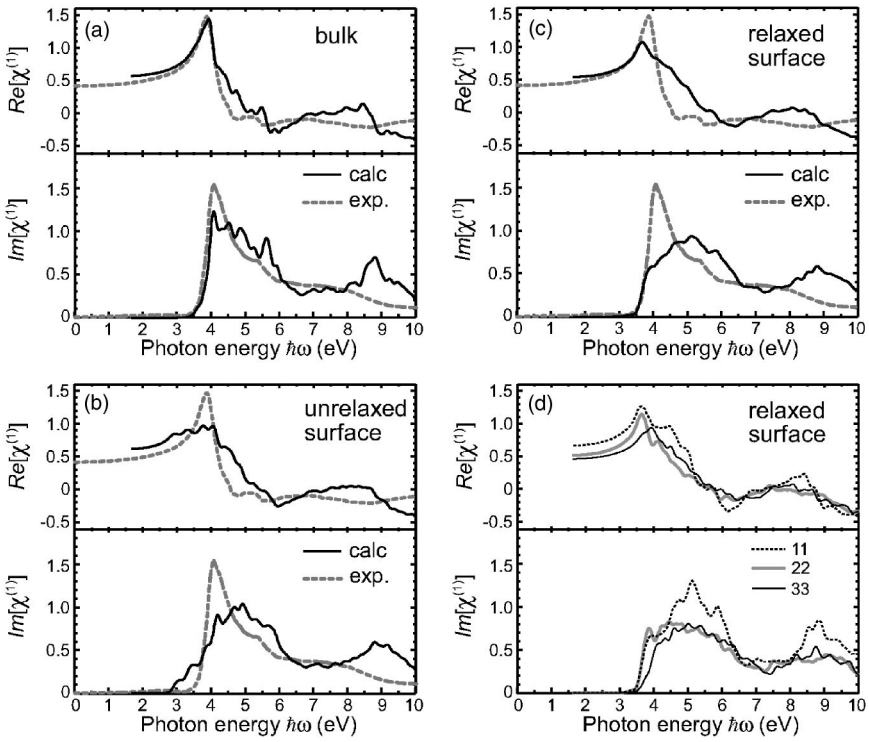

FIG. 4. Calculated linear optical susceptibility $\chi^{(1)}$ as a function of the photon energy for (a) bulk TiO_2, (b) unrelaxed, and (c), (d) relaxed $TiO_2(110)$ surfaces [black solid lines in (a)–(c)]. Gray dashed lines in (a)–(c) represent experimental bulk data of Ref. 39. Black dashed, gray solid, and black solid lines in (d) are susceptibility components of $\chi^{(1)}_{11}, \chi^{(1)}_{22}$, and $\chi^{(1)}_{33}$, where the axes 1, 2, and 3 are defined in Fig. 1.

method. The Fresnel factors for both input and output fields were obtained by a conventional electromagnetic calculation of the light propagation in the stacked dielectric layers. In this electromagnetic calculation, the angle of the incident light beam was 45° from the surface normal, and the linear optical properties from the *ab initio* calculation of the TiO_2 slab structure were used as the dielectric functions of the surface and bulk layers.

We have checked the convergence of the SHG calculation with respect to the number of ***k*** points, the thickness of the vacuum layer, and the number of slab layer (N_{slab}). Calculations using 6, 32, and 64 special ***k*** points in the irreducible Brillouin zone indicate that the curves of the nonlinear susceptibility ($\chi^{(2)}$) as a function of the incident photon energy for 32 and 64 ***k*** points were quite similar to each other, but were significantly different from that obtained for 6 ***k*** points. The calculated curves of $\chi^{(2)}$ for the thickness of the vacuum layer of 5.00 and 8.47 Å were also quite similar to each other. Calculations for $N_{\mathrm{slab}}=3,5$, and 7 indicate that the curves of $\chi^{(2)}$ for $N_{\mathrm{slab}}=5$ and 7 were similar to each other, but were different from that for $N_{\mathrm{slab}}=3$. It follows from these results that good convergence of the electronic level calculation for SH response was achieved using 32 special ***k*** points, a thickness of the vacuum layer of 8.47 Å, and a 7 layer surface model.

III. RESULTS AND DISCUSSION

A. Electronic band structure

The calculated surface electronic band structures of the unrelaxed and relaxed surfaces are shown in Figs. 2(a) and 2(b). A minimum direct band gap is clearly seen at $\bar{\Gamma}$ in Fig. 2(b). The calculated densities of states (DOS) of the unrelaxed and relaxed surfaces are shown in Figs. 3(a) and 3(b). Black solid lines represent the total DOS, gray solid lines, black dashed lines, and gray dashed lines represent the partial DOS of all oxygen atoms, all titanium atoms, and the bridging oxygen [O(1)], respectively. The DOS of the unrelaxed and relaxed surfaces are roughly similar to each other. However, in the DOS of the unrelaxed surface one can see two distinct peaks assigned to the bridging oxygen at the top of the valence band and at the energy of −15 eV. In the case of the relaxed surface, corresponding peaks are moved to lower energies, and the DOS of O(1) exhibit a peak at an energy of about 1 eV below the top of the valence band as indicated by arrows in Fig. 2. This peak shift indicates that the surface relaxation reduces the energy of the bridging oxygen O(1), and consequently widens the surface band gap.

B. Linear optical properties

Figure 4 shows the calculated linear optical susceptibility of the bulk system, and the unrelaxed and relaxed surfaces as a function of the photon energy [black solid lines in Figs. 4(a)–4(c)]. Black dashed, gray solid, and black solid lines in Fig. 4(d) are the calculated susceptibility components of $\chi^{(1)}_{11}$, $\chi^{(1)}_{22}$, and $\chi^{(1)}_{33}$, respectively. Although a rutile TiO_2 crystal has anisotropic optical properties as shown in Fig. 4(d), the curves in Figs. 4(a)–4(c) represent the average of the three susceptibility components $\chi^{(1)}_{xx}$, $\chi^{(1)}_{yy}$, and $\chi^{(1)}_{zz}$ for both experiment and calculation for simplicity. The susceptibility components calculated for the surface models contain both bulk and surface contributions. For comparison, the measured $\chi^{(1)}$ of bulk rutile TiO_2 (Ref. 39) are shown as gray dashed lines in Figs. 4(a)–4(c). The calculated curves, in particular the one for the bulk system, reproduce the structure of the experimental data. Especially, as shown in Figs. 4(a) and 4(c),

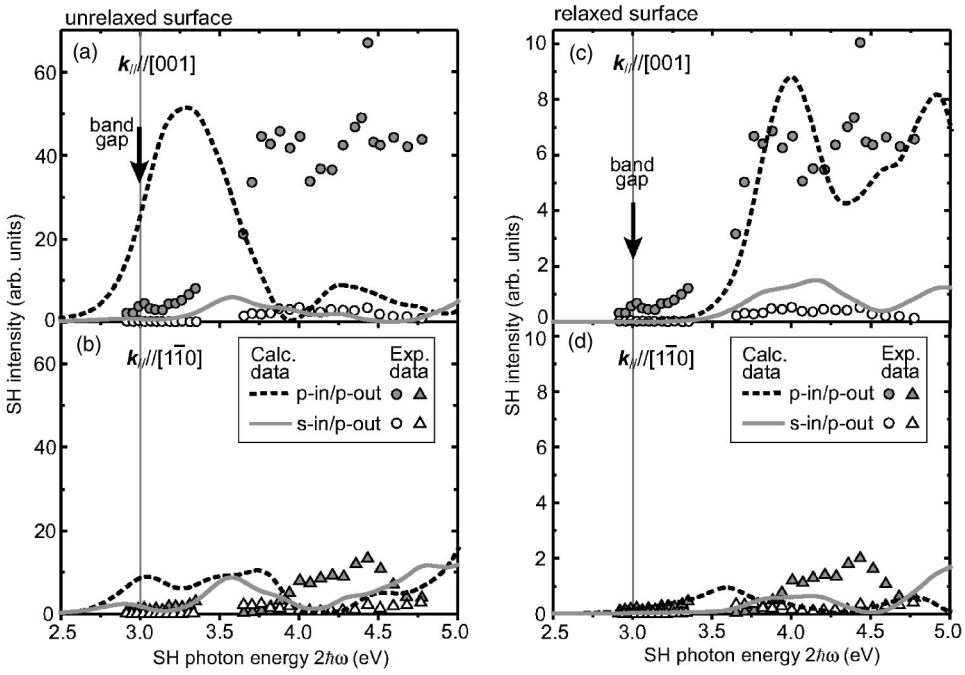

FIG. 5. Calculated SH intensity as a function of the SH photon energy in *p*-in/*p*-out (dashed lines) and *s*-in/*p*-out (gray lines) polarization configurations for (a),(b) unrelaxed and (c),(d) relaxed TiO_2(110) surfaces. The plane of incidence is parallel to the [001] direction for (a),(c), and parallel to the [1$\bar{1}$0] direction for (b),(d). Circles and triangles are measured data of Ref. 15. The scale of the measured data is adjusted as matching with the calculated data.

the structure of the sharp increase of the imaginary part of the calculated $\chi^{(1)}$, i.e., the optical absorption edge around 3.5 eV, agrees well with the measured data. In the case of the unrelaxed surface, the imaginary part of the calculated $\chi^{(1)}$ around 3 eV is larger than the measured data. Since this optical absorption around 3 eV disappears when the surface is relaxed, it results from the surface electronic states of the unrelaxed surface. The DOS of the unrelaxed surface in Fig. 3(a) indicates that this optical absorption around 3 eV originates from the transition from the electronic level of the bridging surface oxygen [O(1)] at the top of the valence band to the bottom of the conduction band.

C. Second harmonic response

Second harmonic light intensity from crystalline materials depends on the polarization of input (fundamental) and output (SH) light, and on the direction of the incident light beam. For the following discussion, the terminology applied for these geometric parameters are defined here. The polarization configurations of input and output fields are described by the notation *p*-in/*s*-out or PS, indicating that input and output polarizations are *p* and *s*, respectively. The symbols *p* or *s* denote the polarization of the electric field of light being parallel or perpendicular to the plane of incidence, respectively. For describing the azimuthal direction of the incident light beam, we use a terminology such as $\boldsymbol{k}_{//}$//[110], where $\boldsymbol{k}_{//}$ is the component of the incident wave vector parallel to the surface plane.

Figure 5 shows the calculated SH intensity as a function of the SH photon energy $2\hbar\omega$ in *p*-in/*p*-out (dashed lines) and *s*-in/*p*-out (gray lines) polarization configurations for the unrelaxed and relaxed TiO_2(110) surfaces. The upper panels [(a) and (c)] and the lower panels [(b) and (d)] of Fig. 5 show the cases with the plane of incidence parallel to [001] and [1$\bar{1}$0] directions, respectively.

Omote *et al.* measured the SH response of the rutile TiO_2(110) surface in air.[15] By x-ray photoemission spectroscopy, they found that some water molecules are physically adsorbed on the sample surface. Since the TiO_2(110) surface is inert, the effect of physisorption of water molecules on surface electronic states is expected to be small. We are using the experimental SHG data of Omote *et al.*[15] (circles and triangles in Fig. 5) for tentative comparison with our calculated results. The measured SH spectra in Fig. 5 indicate that the SH intensity shown as dark circles (we will call this measurement configuration $\boldsymbol{k}_{//}$//[001]-PP) is much larger than that in the other three measurement configurations, and it sharply increases around $2\hbar\omega$=3.5 eV. These features are well reproduced by the calculated SH intensity of the relaxed surface as seen in Figs. 5(c) and 5(d). On the other hand, Fig. 5(a) shows that the calculated SH intensity of the unrelaxed surface in the $\boldsymbol{k}_{//}$//[001]-PP configuration is quite different from the measured data.

In general, the linear optical susceptibility $\chi^{(1)}$ as well as the nonlinear optical susceptibility $\chi^{(2)}$ affect the shape of the SH spectra through the Fresnel factors. Therefore, the sharp rise of the SH intensity at $2\hbar\omega$=3.5 eV in the $\boldsymbol{k}_{//}$//[001]-PP configuration may reflect only the spectral shape of the linear optical properties. However, we confirmed that the calculated nonlinear susceptibility components drastically increase at $2\hbar\omega$=3.5 eV. For the sake of conciseness, these detailed computational results are not shown here. It is revealed that the spectral shape in the $\boldsymbol{k}_{//}$//[001]-PP configuration essentially results from the surface SH response. The origin of the large surface SH response around $2\hbar\omega$=4 eV is discussed below.

In Fig. 5 we see a significant difference in the surface SH response between the unrelaxed and relaxed surfaces, while the difference in the linear optical properties between the two surfaces is rather small as shown in Fig. 4. This indicates that SHG is more sensitive to the surface electronic states and to

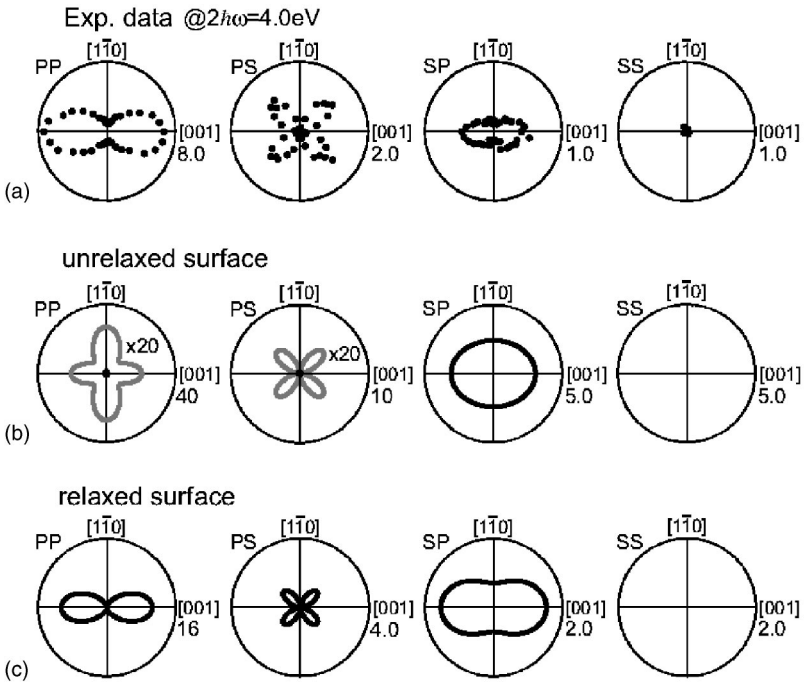

FIG. 6. SH intensity as a function of the sample rotation angle around the surface normal at the SH photon energy $2\hbar\omega=4.0$ eV: (a) experimental data of Ref. 15, (b) calculated patterns for unrelaxed surface, and (c) calculated patterns for relaxed surface. PP, PS, SP, and SS represent the polarization configurations of input and output fields. The units of the radial direction are arbitrary units.

the surface structure than the linear optical response so far as the TiO_2 surface is concerned.

Figure 6 shows the SH intensity as a function of the sample rotation angle around its surface normal at the SH photon energy $2\hbar\omega=4$ eV, where an outstandingly large SH intensity is observed. Experimental data[15] and calculated results of the unrelaxed and relaxed surfaces are presented in Figs. 6(a), 6(b), and 6(c), respectively. The angle patterns in Fig. 6 reflect the anisotropy of the SH response in the surface plane. The calculated shapes of angle patterns and the relative SH intensity between the polarization configurations of the relaxed surface agree well with the experimental data. On the other hand, the calculated results of the unrelaxed surface do not agree with the measured data. Summarizing the results shown in Figs. 5 and 6, we conclude that the calculated SH intensity from the relaxed surface reproduces the measured data much better than that from the unrelaxed surface, and reasonable SH response of TiO_2 surface was obtained by the applied *ab initio* method.

Further deepening our analysis, we discuss the origin of the large SH response of the $TiO_2(110)$ surface around $2\hbar\omega=4$ eV. Because the valence and conduction bands of TiO_2 are mostly composed from electronic states of oxygen and titanium character, respectively, as shown in Fig. 3, the electronic transitions between oxygen and titanium states are considered as important for the optical response at $2\hbar\omega=4$ eV. Thus, we examined the SH response of various Ti-O pairs on the surface. As shown in Fig. 7(e), the surface of rutile $TiO_2(110)$ consists of four atomic sites, i.e., bridging oxygen [O(1)], in-plane oxygen [O(2)], sixfold coordinated titanium [Ti(1)], and fivefold coordinated titanium [Ti(2)]. There are three pairs of Ti and O atoms adjacent to each other: O(1)-Ti(1), O(2)-Ti(1), and O(2)-Ti(2). We separated the SH response of the electronic states, satisfying the condition that their wave functions are localized in one of the Ti-O pairs. In this procedure, eigenstates localized in one of the Ti-O pairs were selected by evaluating the electron charge density inside each atomic sphere for each eigenstate. The nonlinear susceptibility components were then calculated exclusively from these selected eigenfunctions, containing both localized components inside atomic spheres and non-localized components in the interstitial region. Figures 7(b)–7(d) show the calculated SH intensity as a function of the sample rotation angle around its surface normal in *p*-in/*p*-out polarization configuration at $2\hbar\omega=4$ eV for the O(1)-Ti(1), O(2)-Ti(1), and O(2)-Ti(2) pairs, respectively. The experimental data are presented in Fig. 7(a). The comparison in Fig. 7 demonstrates that the calculated pattern of the O(1)-Ti(1) pair agrees well with the measured pattern,

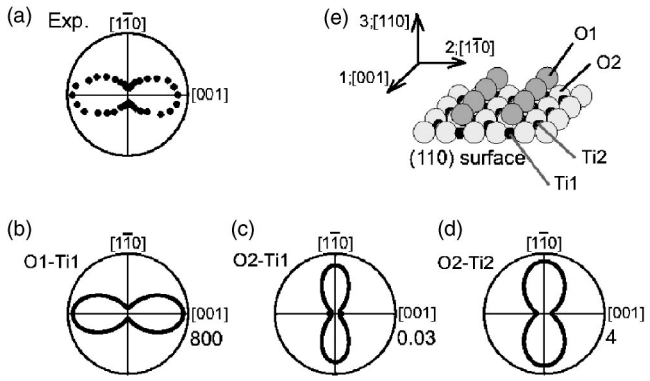

FIG. 7. SH intensity as a function of the sample rotation angle around the surface normal in *p*-in/*p*-out polarization configuration at $2\hbar\omega=4.0$ eV: (a) experimental data of Ref. 15, (b)–(d) the calculated SH responses from the electronic states localized in (b) bridging oxygen O(1) and six-fold coordinated Ti(1), (c) in-plane oxygen O(2) and Ti(1), and (d) O(2) and five-fold coordinated Ti(2). The units of the radial direction are arbitrary units. Panel (e) shows sites of oxygen and titanium [O(1), O(2), Ti(1), and Ti(2)] on the clean $TiO_2(110)$ surface.

while the other two calculated patterns do not, and the SH intensity of the O(1)-Ti(1) pair is more than a few hundred times larger than those of the other pairs. Although Ti and O atoms below the surface also contribute to the total surface SH response, their contribution drastically decreases as they are located deeper in the bulk for the case of a centrosymmetric material like a TiO_2 crystal. Therefore, we conclude that the Ti-O zigzag chains consisting of bridging oxygen O(1) and sixfold coordinated Ti(1) on the surface dominantly contribute to the SH response of the $TiO_2(110)$ surface around $2\hbar\omega=4$ eV.

Finally, we consider the origin of the large difference in SH intensity between the O(1)-Ti(1) pair and the other pairs. This difference can be qualitatively explained based on the polarizable-bond model.[40] Assuming that the SH response due to the electronic transition between Ti and O atoms is expressed by SH dipoles induced in the Ti-O bonds, the SH responses from the O(1)-Ti(1), O(2)-Ti(1), and O(2)-Ti(2) pairs can be described by the SH dipoles as shown in Fig. 8. Figure 8(a) shows that SH dipoles corresponding to the O(1)-Ti(1) bonds form the total SH dipole parallel to the surface normal, so that it emits strong SH light. On the other hand, since SH dipoles corresponding to the O(2)-Ti(1) or O(2)-Ti(2) bonds are oriented in the opposite directions as shown in Figs. 8(b) and 8(c), the total amount of them becomes very small by cancellation, and it emits weak SH light. Thus we see that orientation and symmetry of Ti-O bonds cause the difference of SH intensity.

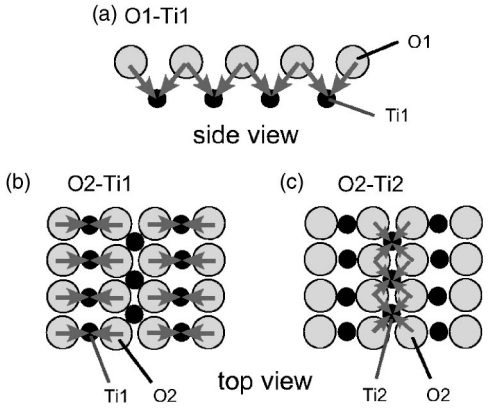

FIG. 8. Polarizable-bond models for the SH responses of (a) O(1)-Ti(1), (b) O(2)-Ti(1), and (c) O(2)-Ti(2) bonds. Arrows represent the SH dipoles induced in each Ti-O bond. For the sake of a clear illustration, circles corresponding to O(1) are removed in (b) and (c).

IV. CONCLUSION

We have calculated the SH intensity from rutile $TiO_2(110)$ surface by the *ab initio* FLAPW method. The calculated SH spectra and azimuthal angle dependence of the SH intensity for the relaxed surface reproduce the experimental data.[15] The analysis of our *ab initio* data suggests that the Ti-O zigzag chains of the $TiO_2(110)$ surface make the dominant contribution to the large surface SH response around $2\hbar\omega=4$ eV.

ACKNOWLEDGMENTS

This work was supported by a Grant-in-Aid for Scientific Research from the Ministry of Education, Culture, Sports, Science, and Technology of Japan. We also gratefully acknowledge support by the Austrian Science Fund (FWF) by Project No. S9008-N02.

*Electronic address: h-sano@jaist.ac.jp

[1] A good general review of surface science of TiO_2 has been given by U. Diebold, Surf. Sci. Rep. **48**, 53 (2003).
[2] G. Charlton, P. B. Howes, C. L. Nicklin, P. Steadman, J. S. G. Taylor, C. A. Muryn, S. P. Harte, J. Mercer, R. McGrath, D. Norman, T. S. Turner, and G. Thornton, Phys. Rev. Lett. **78**, 495 (1997).
[3] B. Hird and R. A. Armstrong, Surf. Sci. **385**, L1023 (1997).
[4] B. Hird and R. A. Armstrong, Surf. Sci. **420**, L131 (1999).
[5] U. Diebold, J. Lehman, T. Mahmoud, M. Kuhn, G. Leonardelli, W. Hebenstreit, M. Schmid, and P. Varga, Surf. Sci. **411**, 137 (1998).
[6] K. I. Fukui, H. Onishi, and Y. Iwasawa, Phys. Rev. Lett. **79**, 4202 (1997).
[7] R. Heise, R. Courths, and S. Witzel, Solid State Commun. **84**, 599 (1992).
[8] P. J. Hardman, G. N. Raikar, C. A. Muryn, G. van der Laan, P. L. Wincott, G. Thornton, D. W. Bullett, and P. A. D. M. A. Dale, Phys. Rev. B **49**, 7170 (1994).
[9] A. K. See, M. Thayer, and R. A. Bartynski, Phys. Rev. B **47**, 13722 (1993).
[10] L. Soriano, M. Abbate, J. Vogel, J. C. Fuggle, A. Fernandez, A. R. Gonzalez-Elipe, M. Sacchi, and J. M. Sanz, Surf. Sci. **290**, 427 (1993).
[11] A. N. Shultz, W. Jang, W. M. Hetherington, III, D. R. Baer, L-Q. Wang, and J H. Engelhard, Surf. Sci. **339**, 114 (1995).
[12] E. Kobayashi, G. Mizutani, and S. Ushioda, Jpn. J. Appl. Phys., Part 1 **36**, 7250 (1997).
[13] E. Kobayashi, T. Wakasugi, G. Mizutani, and S. Ushioda, Surf. Sci. **402–404**, 537 (1998).
[14] G. Mizutani, N. Ishibashi, S. Nakamura, T. Sekiya, and S. Kurita, Int. J. Mod. Phys. B **15**, 3873 (2001).
[15] M. Omote, H. Kitaoka, E. Kobayashi, O. Suzuki, K. Aratake, H. Sano, G. Mizutani, W. Wolf, and R. Podloucky, J. Phys.: Condens. Matter (to be published).
[16] A review of recent *ab initio* calculations of surface SHG has been given by H. Sano and G. Mizutani, e-J. Surf. Sci. Nanotech. **1**, 57 (2003).
[17] D. Lim, M. C. Downer, J. G. Ekerdt, N. Arzate, B. S. Mendoza, V. I. Gavrilenko, and R. Q. Wu, Phys. Rev. Lett. **84**, 3406 (2000).
[18] V. I. Gavrilenko, R. Q. Wu, M. C. Downer, J. G. Ekerdt, D. Lim, and P. Parkinson, Phys. Rev. B **63**, 165325 (2001).
[19] J. E. Mejia, B. S. Mendoza, M. Palummo, G. Onida, R. Del Sole,

S. Bergfeld, and W. Daum, Phys. Rev. B **66**, 195329 (2002).
[20] H. Sano, G. Mizutani, W. Wolf, and R. Podloucky, Phys. Rev. B **66**, 195338 (2002).
[21] N. N. Dadoenkova, T. Andersen, and W. Hübner, Appl. Phys. B: Lasers Opt. **74**, 705 (2002).
[22] K. M. Glassford and J. R. Chelikowsky, Phys. Rev. B **46**, 1284 (1992).
[23] Shang-Di Mo and W. Y. Ching, Phys. Rev. B **51**, 13023 (1995).
[24] D. Vogtenhuber, R. Podloucky, A. Neckel, S. G. Steinemann, and A. J. Freeman, Phys. Rev. B **49**, 2099 (1994).
[25] M. Ramamoorthy, D. Vanderbilt, and R. D. King-Smith, Phys. Rev. B **49**, 16721 (1994).
[26] P. Reinhardt and B. A. Hess, Phys. Rev. B **50**, 12015 (1994).
[27] S. P. Bates, G. Kresse, and M. J. Gillan, Surf. Sci. **385**, 386 (1997).
[28] P. K. Schelling, N. Yu, and J. W. Halley, Phys. Rev. B **58**, 1279 (1998).
[29] N. M. Harrison, X. -G. Wang, J. Muscat, and M. Scheffler, Faraday Discuss. **114**, 305 (1999).
[30] H. J. F. Jansen and A. J. Freeman, Phys. Rev. B **30**, 561 (1984).
[31] E. Wimmer, H. Krakauer, M Weinert, and A. J. Freeman, Phys. Rev. B **24**, 864 (1981).
[32] G. Kresse and J. Furthmüller, Comput. Mater. Sci. **6**, 15 (1996); Phys. Rev. B **54**, 11169 (1996); G. Kresse and D. Joubert, *ibid.* **59**, 1758 (1999).
[33] L. Hedin and B. I. Lundqvist, J. Phys. C **4**, 2064 (1971).
[34] L. Hedin and S. Lundqvist, J. Phys. (Paris), Colloq. **33**, C3-73 (1972).
[35] D. J. Singh, *Planewaves, Pseudopotentials and the LAPW Method* (Kluwer Academic Publishers, Boston, 1994), pp. 73–76.
[36] H. J. Monkhorst and J. D. Pack, Phys. Rev. B **13**, 5188 (1976).
[37] L. Hedin, J. Phys.: Condens. Matter **11**, R489 (1999).
[38] B. S. Mendoza, M. Palummo, G. Onida, and R. Del Sole, Phys. Rev. B **63**, 205406 (2001).
[39] M. Cardona and G. Harbeke, Phys. Rev. **137**, A1467 (1965).
[40] B. S. Mendoza and W. L. Mochan, Phys. Rev. B **55**, 2489 (1997).